

See discussions, stats, and author profiles for this publication at: <https://www.researchgate.net/publication/280133315>

# Mission Design and Concept of Operations of a 6U CubeSat Mission for Proximity Operations and RSO Imaging

Conference Paper · May 2013

CITATIONS

0

READS

1,192

13 authors, including:



**Bogdan Udrea**

Embry-Riddle Aeronautical University

62 PUBLICATIONS 199 CITATIONS

[SEE PROFILE](#)



**Michael V Nayak**

17 PUBLICATIONS 83 CITATIONS

[SEE PROFILE](#)



**Paryus Patel**

Prime Healthcare

112 PUBLICATIONS 2,798 CITATIONS

[SEE PROFILE](#)



**Adam Huang**

University of Arkansas

45 PUBLICATIONS 664 CITATIONS

[SEE PROFILE](#)

Some of the authors of this publication are also working on these related projects:



A pivotal signalling molecule in neurodegeneration [View project](#)

## **Mission Design and Concept of Operations of a 6U CubeSat Mission for Proximity Operations and RSO Imaging**

B. Udrea<sup>1</sup>, M. Nayak<sup>2</sup>, M. Ryle<sup>1</sup>, N. Martini<sup>1</sup>, S. Gillespie<sup>1</sup>, T. Grande<sup>1</sup>, S. Caicedo<sup>1</sup>, S. Willette<sup>1</sup>, A. Baba<sup>1</sup>, K., Harris<sup>1</sup>, J. DiGregorio<sup>1</sup>, S. Salzburger<sup>1</sup>, P. Patel<sup>1</sup>, A. Huang<sup>3</sup>

<sup>1</sup>Embry-Riddle Aeronautical University, 600 S. Clyde Morris Blvd, Daytona Beach, FL 32114, 386-226-6630, [udreab@erau.edu](mailto:udreab@erau.edu) ;

<sup>2</sup>Space Development and Test Directorate, Kirtland AFB, 3656 Aberdeen Ave SE, Albuquerque, NM 87106, 505-853-3656, [michael.nayak@gmail.com](mailto:michael.nayak@gmail.com);

<sup>3</sup>University of Arkansas, 863 W. Dickson St., MEEG 105, Fayetteville, AR 72701, 479-575-7485, [phuang@uark.edu](mailto:phuang@uark.edu)

ARAPAIMA is a proximity operations mission sponsored by the US Air Force Office of Scientific Research and the Air Force Research Laboratory, to perform the in-orbit demonstration of proximity operations for visible, infrared, and three dimensional imaging of resident space objects (RSOs) on a nanosat platform. The nanosat is of the 6U CubeSat class, with overall dimensions of 11×26×34cm and a mass of 9kg. This paper details the goals and the concept of operations of the mission and presents the current status of the design.

**Keywords:** *proximity, operations, imaging, agile, cubesat*

### **1. Introduction**

The mission discussed in this paper is an ongoing project at the Embry-Riddle Aeronautical University (ERAU) Spacecraft Development Laboratory (SDL) and is sponsored by the US Air Force Office of Scientific Research (AFOSR) and the Air Force Research Laboratory (AFRL) University Nanosat Program (UNP). The Application for RSO Autonomous Proximity Analysis and IMAGING (ARAPAIMA) is a three-axes stabilized nanosat of the 6U class, with an overall size of 11×26×34cm and a mass of 9kg. The only significant difference between the nanosat and a large, typical, satellite is the lack of redundant components in the attitude determination and control subsystem (ADCS). The goal of the mission is to test nanosat technologies for the performance of space-based space situational awareness (SSA) tasks.

The concept of operations (ConOps), illustrated in Figure 1, has three *gates* which correspond to the minimum, full, and extended mission success criteria. The first gate (minimum success criterion) is to successfully take an unresolved image of the RSO and downlink it to the ground station. For the purpose of the ARAPAIMA mission the upper stage that releases the nanosat is employed as a surrogate RSO. The second

gate (full mission success criterion) is to maneuver the nanosat into the proximity of the RSO, with commands generated by the mission operators, and take an image in which the RSO occupies at least 15% of the pixels of the visible and IR spectrum cameras.

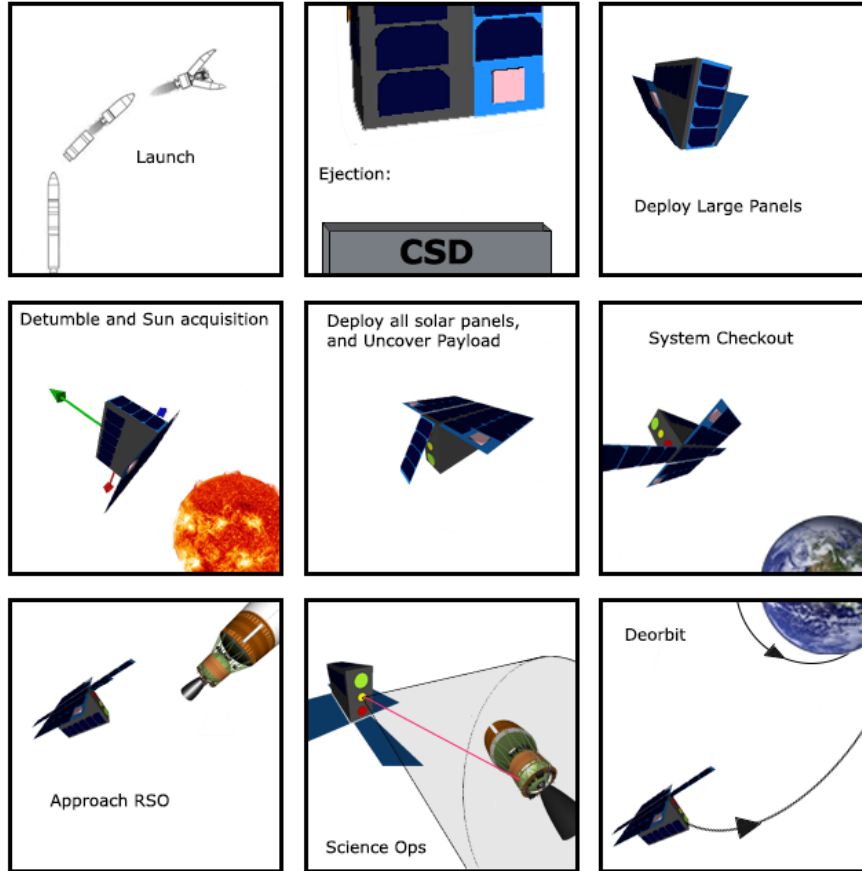


**Figure 1:** ARAPAIMA concept of operations. simulations have shown encouraging results.

The third gate (extended mission success criterion) is the on-board planning and execution of maneuvers to acquire a relative orbit with respect to the RSO and use the LRF to generate a 3D point cloud.

The approach to the design of the ARAPAIMA mission closely follows that of a fully fledged science mission. The basic concept has been developed into the design of the experiment and initial

## 2. Spacecraft Design

The results of the first iteration of the preliminary design are described in this section together with salient engineering details and current design status. Components of all the nanosat subsystems have been selected and the majority have been modeled in CATIA. A 3D model of the nanosat and mass, power, data, and link budgets have been generated and are continuously revised and updated. A functional diagram of the nanosat is presented in Figure 2 and the 3D rendering of the most recent (MkX) version of the design is shown in Figure 3.

### 2.1. Nanosat Subsystems and Components

The satellite is a three-axis stabilized nanosat, of  $11 \times 26 \times 34$ cm overall dimensions, that classifies as a 6U CubeSat. The launch mass is 9kg which includes 1kg of propel-

land and it is padded with generous component and system margins.

During nominal operations the nanosat uses its star tracker (STR) for attitude determination and a set of three reaction wheels (RWs) for attitude control. The RWs produce attitude control torques for both slewing the nanosat and to reject perturbations due to aerodynamic forces, gravity gradient, and solar radiation pressure (SRP). The reaction control system (RCS) thrusters produce torques to unload the reaction wheels. The S3S star tracker and the RW-0.03-4 reaction wheels, which have been selected for the ARAPAIMA mission, are manufactured and distributed by Sinclair Interplanetary and they seem, for the time being, to offer the best price-performance combination on the market. The manufacturer quoted accuracy of the S3S is 7 $\mu$ s normal to the STR optical axis and 70 $\mu$ s about the optical axis. In the current configuration the STR baffle provides an exclusion half-angle of 30°. The STR is installed so that its optical axis is anti-parallel with the optical axes of the payload instruments.

The RW-0.03-4 reaction wheel produces a nominal torque of 2mNm and it can store an angular momentum of 30mNm $\cdot$ s at 5600RPM. The RWs are installed so that their axes of rotation are mutually perpendicular and closely aligned with the nanosat body axes. An inertial measurement unit (IMU), consisting of two triads of mutually perpendicular accelerometers and rate gyroscopes is also part of the guidance, navigation, and control (GNC) suite. During the de-

tumble phase the STR can only produce accurate attitude solutions when the angular rates are below a few degrees per second per axis. Thus the angular rates are measured by the gyros and brought to zero by the RCS thruster torques during the de-tumble mode. The output of the IMU is monitored during nominal operations to detect any anomalous angular rates or accelerations and trigger a fault mode. The nanoIMU from MEMSense has been chosen for ARAPAIMA for its small size and based on the experience of the ARAPAIMA design team and CubeSat component manufacturers. A Novatel OEMV-1 GPS receiver and its patch antenna complete the guidance, navigation, and control suite (GNC) and provides positioning, navigation, and timing (PNT)

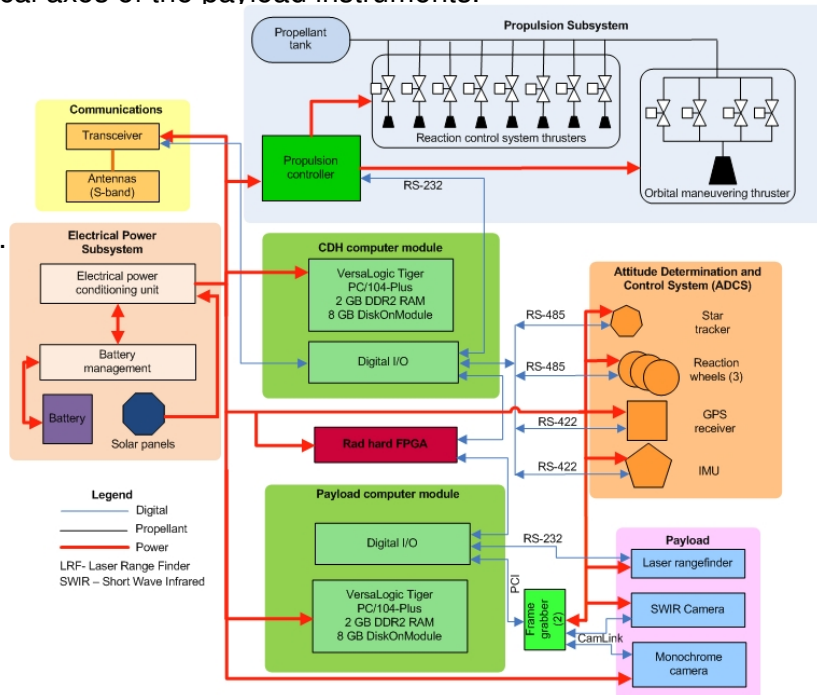


**Figure 2:** ARAPAIMA nanosat functional architecture. The nanosat has the same complement of subsystems as a regular three-axis stabilized satellite.

functions. The dynamic restrictions of the receiver will be removed by installing a vendor provided software patch prior to the receiver integration with the flight model of the nanosat.

The instruments of the payload are an MLR2K rangefinder from FLIR Systems Inc., a short wave (SW) IR camera from Goodrich Aerospace Inc., and a monochrome visible spectrum camera from SenTech, Ltd. Due to the high computational load of the payload it has been decided to fly a dedicated payload computer based on an Intel 32bit processor. Two frame grabbers one for each camera, will be used to connect the cameras to the payload computer module. Details of the payload science, the instruments, and preliminary results of the laboratory characterization of a payload emulator are presented in Section 3.

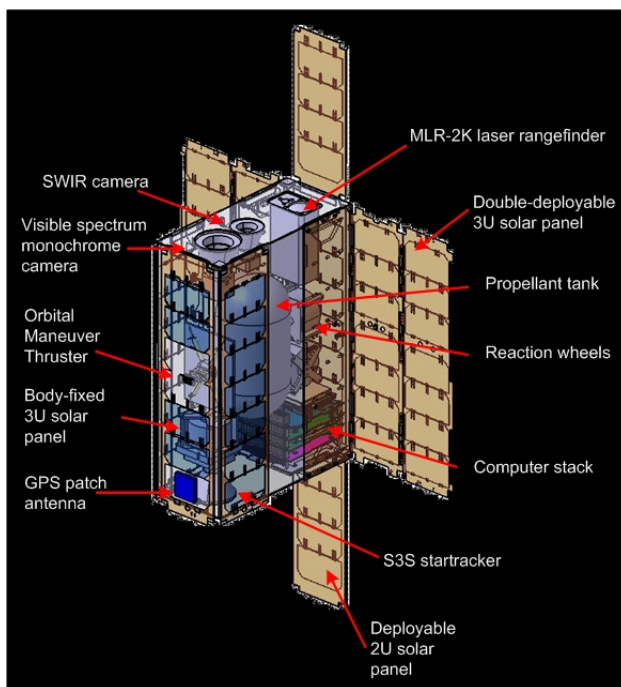


**Figure 3:** Rendering of the MkX version of the ARAPAIMA 6U CubeSat.

The command, control, and communications (C3) subsystem consists of an S-band radio, two patch antennas, and an on-board computer (OBC). The Cadet radio from L3 Communications has been chosen because it fits the ARAPAIMA's 6U form factor and it utilizes relatively low power. It already has flight heritage on the CINEMA mission that has recently launched. The radio operates in the S-band (around the 2.2GHz band) for downlink, and in the UHF-band (around 440MHz) for uplink, it utilizes a half-duplex architecture, and it is capable of providing up to 10Mbps downlink and 250kbps uplink bandwidths. The radio has a large data buffer, 4GB, which makes it a good choice for a store and forward communications architecture. The data buffer of the radio can store, for example, over 1000 images of  $640 \times 512$  pixels taken at 12 bit depth with the IR camera. The radio supports the commercial grade Advanced Encryption Standard (AES) with a 256bit key. For the time being the patch antennas are placed on the deployable solar panels satellite, at a center to center distance of 25cm. The antennas will

The propulsion subsystem consists of eight RCS thrusters and one orbital maneuvering thruster (OMT) thruster. The RCS thrusters (not shown in Figure 3) are installed such that they produce control torques in both positive and negative directions about each body axis. During orbital maneuvers the attitude control is performed in closed loop with the RCS thrusters which are commanded with pulse width modulation (PWM) signals. The propulsion subsystem is an enabling technology and it is described in detail in Section 2.2.

The command, control, and communications (C3) subsystem consists of an S-band radio, two patch antennas, and an on-board computer (OBC). The Cadet radio from L3 Communications

be checked for interference in the course of the subsequent design iterations. During the communication phases of the mission the nanosat will be commanded such that the face with the antennas points in the nadir direction. To close the communication link a ground station with an unsophisticated S-band antenna can provide a bandwidth of up to 10kbps to a small patch antenna in LEO. A more advanced ground station with a 1m parabolic dish can provide bandwidths of 1Mbps and better.

The OBC is the same model as the payload computer. The choice reduces the risk for the on-board software development (OSW) and increases the reliability of the computer architecture by providing the means to implement dual computer redundancy. Due to the critical aspect of proximity operations it has been decided to fly a simple and inexpensive dual redundant system made of two VersaLogic Tiger PC/104-Plus CPU modules, one for the payload computer and the other for the C3 computer.

In the current design the CPU modules are connected to a radiation hardened FPGA. The FPGA runs a simple but robust supervisory routine and safe mode controller and periodically stores the state vector of the nanosat subsystems. In the event of a fault in the C3 computer the supervisor on the FPGA triggers the safe mode controller and attempts to restart the C3 computer. If the C3 computer cannot be started the supervisor transfers the control of the nanosat to the payload computer and it loads the flight control software on it.

The electrical power subsystem (EPS) of the MkX configuration consists of five solar panels, a battery, and an electrical power conditioning/battery charging unit. Two large deployable solar panels of 20×30cm carry 13 solar cells each and two smaller deployable solar panels carry four solar cells each. Three body-fixed 25×30cm solar panel carry 15 solar cells. The two smaller deployable solar panels also serve as aperture covers for the payload instruments and the star tracker when the nanosat is in storage and during launch and detumble. A power regulation/battery charging module and two 30Wh batteries complete the EPS. The solar panels, power module, and the batteries will most likely be procured from Clyde Space.

**Table 1:** Components of the ARAPAIMA nanosat and their TRLs. The components not available off-the-shelf are highlighted.

	Components	TRL	Heritage
1	Reaction wheel	9	numerous
2	Star tracker	6	BRITE, Nov. 2012 <sup>a</sup>
3	IMU	7-8	Colony 2
4	GPS receiver	9	RAX, Nov. 2010
5	Power cond. module	9	numerous
6	Solar panels	9	numerous
7	Battery	9	numerous
8	On-board computer	6-7	Oculus
9	Radio	9	CINEMA, Sep. 2012
10	S-band antenna	7-8	numerous
11	Mini rangefinder	5	none
12	IR camera	5	none
13	Payload computer	6	ARC, TBA
14	RCS thrusters	5-6	U Ark <sup>b</sup>
15	OMT	5-6	U Ark <sup>c</sup>
16	Propellant tank	6-7	ERAU, U Ark
<sup>a</sup> launch delayed			
<sup>b</sup> with NASA Marshall			
<sup>c</sup> with AFRL (RAMPART)			

The thermal control subsystem has not been specified during the first design iteration. The specification of its requirements are pending consolidation of the design of the nanosat. However, it is expected that it will consist of passive thermal control means such as insulators and paints and possibly heaters for the control of the temperature for sensitive components such as batteries. A thorough thermal analysis using a lumped capacitance model is planned for the preliminary design review (PDR) and a full finite element model (FEM) analysis for the critical design review (CDR).

The ARAPAIMA mission operators will execute the DoD Instruction 3100.12 [1] that requires minimization of space debris (Section 6.3) and planning for the spacecraft end-of-life operations (Section 6.4). Since ARAPAIMA flies in LEO an atmospheric re-entry is planned as the end-of-life for ARAPAIMA. Support of the Air Force Space Test Program (STP) flight team will be sought for estimating the re-entry survival of components and structural fragments which “*shall not exceed 1 in 10,000.*” as specified in [1]. A worst case scenario has been analyzed to determine the maximum altitude from which the uncontrolled ARAPAIMA re-enters the atmosphere in 25 years or less, as per Section 6.4.1 of DoD Instruction 3100.12. The scenario considers a nanosat with a mass of 9kg that is unresponsive from separation from the launcher. To be conservative the surface area for drag is the smallest cross-sectional area of the nanosat,  $(0.11 \times 0.26) = 0.0286\text{m}^2$ . The SRP area is the next smaller area,  $(0.11 \times 0.3) = 0.033\text{m}^2$ . The drag coefficient,  $C_d$ , is 2.2 and the reflectivity coefficient,  $C_r$ , is 1.0. It has been assumed that the nanosat is in a circular orbit, starting on January 1, 2015 with an inclination of  $28.5^\circ$ . The lifetime tool in STK has been employed to calculate the orbit decay with the default selection of Jacchia’s lifetime atmospheric model and Schatten’s solar flux model. It has been determined that, with the parameters mentioned above, an unresponsive ARAPAIMA will decay from a circular LEO of 535km altitude in 24.7 years. The maximum safe altitude can be raised by venting the 1kg of propellant taken up by ARAPAIMA to reduce the mass of the nanosat to 8kg. A gain of only 15km is realized and the added complexity of a fail-safe propellant venting mechanism and of a zero-thrust relief valve led to the elimination of this option. Based on the analysis described above it has been decided that the maximum altitude of the circular LEO of the ARAPAIMA mission is 500km.

The components of the nanosat, in the current configuration, are shown in Table 1 together with their technology readiness levels (TRL). It is expected that at the time ARAPAIMA is integrated for flight, all the components will have TRL levels between 8 and 9, with the exception of the LRF and IR camera. An aggressive LRF and IR camera testing schedule will seek to bring their TRLs to a level of at least 6 at the time of integration for flight.

The nanosat configuration presented in this section has been generated in parallel with the mission concept described above. Once the nanosat design is frozen the concept of operations will be tested with end-to-end simulations using MATLAB/Simulink/Stateflow and STK. It is expected that the end-to-end simulator will be ready by the CDR (January 2014) and it will be used to refine the concept of operations and take into account the

peculiarities of the 6U nanosat bus and the tight integration of its subsystems.

## 2.2. Propulsion Subsystem

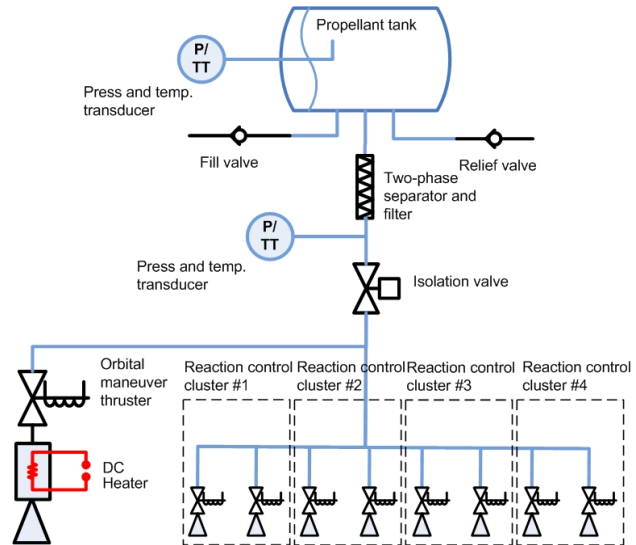
Cold and warm gas thruster science and engineering are well-understood and developed for large satellites (TRL9), operations of which satisfy all the safety and power requirements. To ensure mission success the key challenge of a nanosat propulsion system (NSPS) lies in its miniaturization and integration with the other nanosat subsystems, while maintaining the highest TRL levels of all currently available technologies.

Figure 4 shows the overall system diagram of the proposed NSPS. It utilizes mixed miniaturization technologies, including those of nano/micro-electro mechanical systems (MEMS), high performance commercially-off-the-shelf solenoid valves.

The ultimate expression of a miniaturized satellite is the monolithically fabricated satellite (sensors, actuators, electronics, power, and structure) fashioned after the techniques used for integrated-circuits production through advances in micro- and nano-technologies. However, the technology is not fully mature yet, hence the adoption of hybridized technologies to maximize the TRL of the NSPS for the ARAPAIMA mission. The starting point is based on the near-direct evolutionary technologies of The Aerospace Corporation nanosat propulsion heritage [3], in particular the STS-116 MEPSI and the terrestrial prototypes of the Co-Orbiting Satellite Assistant Propulsion Modules (COSA-PM).

The proposed ARAPAIMA NSPS propellant is based on the DuPont HFC-236fa (1,1,1,3,3,3-Hexafluoropropane,  $I_{sp}=47s$  vacuum,  $p_{25^{\circ}C}=2.7bar$ , specific gravity=1.37) refrigerant/fire-extinguishing agent flown on the AeroCube-2 and tested in the COSA-PM experiments. The propellant is a liquefied gas that provides self-pressurization to the propulsion system.

Specific modifications for ARAPAIMA include the use of silicon micro-fabricated integrated heater-nozzles, isolation valves, and a passive two-phase fluid separator which ensures gas-state-



**Figure 4:** ARAPAIMA NSPS schematic. The OMT is fed by a cluster of valves to achieve the required mass flow rates while each RCS thrusters are each fed by a single valve.

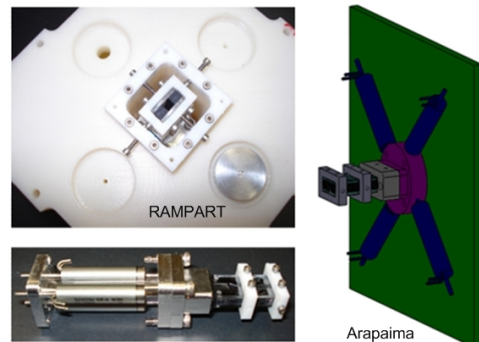


**Figure 5:** RAMPART engineering qualification OMT and rendering of its modification for ARAPAIMA.

only propellant downstream of the propellant tank. A variant of the COTS solenoid valves, as used in the STS-116 MEPSI, and tested in COSA-PM is used for the NSPS RCS thrusters (Lee Valve INKA1222201H). A cluster of four extended performance valves, Lee IEPA1221241H, is used for the OMT feed due to the requirement of higher mass flow rates. The miniature solenoid valves for the NSPS are part of the family of The Lee Company nanoliter dispensing valves often used in liquid droplet handling applications. In the intended, liquid based, applications the valve warranty is for 250 million life cycles. However, for inert fluids, such as the HFC-236fa propellant for ARAPAIMA, the expected life is in excess of 1 billion cycles, equivalent to over 3 years of continuous operations at 10Hz. It is interesting to note that the proposed NSPS is a direct modification of the Rapid-Prototype MEMS Propulsion And Radiation Test (RAMPART) 2U CubeSat currently manifested on the ORS-3 mission, slated for launch no earlier than October 2013. The similarity and differences are shown in Figure 5. The key difference between RAMPART and ARAPAIMA is the inclusion of RCS thrusters for attitude control for agility which is in contrast to RAMPART's passive magnetic stabilization. RAMPART [4] is expected to experience chronic oscillations while ARAPAIMA is fully three-axes stabilized.

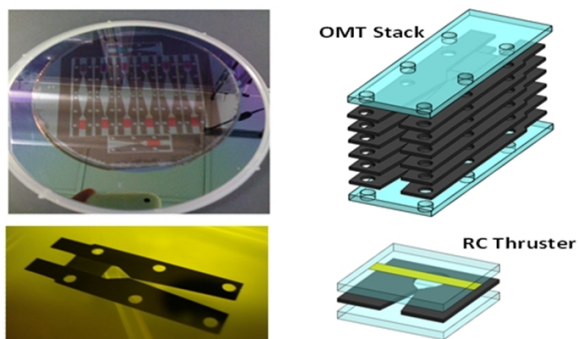


**Figure 6:** The OMT and RCS thruster nozzle assemblies. The dimensions of the OMT and the RCS thruster are  $5.2 \times 10 \times 28\text{mm}$  and  $2.7 \times 1 \times 1\text{mm}$  respectively. Also shown in Figure 6 is the OMT nozzle wafer during the fabrication process and the individual nozzle chips after release from the substrate.

The expected thrust of the RCS thrusters and OMT nozzles are 10mN and 100mN, respectively. The design of the RCS thruster and OMT are shown in Figure 6. Both utilize micro-fabricated deep reactive-ion etching (DRIE) silicon nozzles. The RCD nozzles are capped by Pyrex-glass through anodic bonding and the OCT nozzle stacks are fusion bonded. Also shown in Figure 6 is the OMT nozzle wafer during the fabrication process and the individual nozzle chips

The valve responses are linear to over 100Hz and tri-state to 1kHz. The thruster valves are controlled through pulse-width modulation and have duty range, translating to  $100\mu\text{N}$  and 5mN minimum thrust or  $1\mu\text{N}\cdot\text{s}$  and  $50\mu\text{N}\cdot\text{s}$  impulse bits, for the RCS thrusters and the OMT respectively. *The capability to throttle the OMT presents the opportunity to design more efficient maneuvers than those performed with bang-on/bang-off thrusting only.* With a tank volume of about  $800\text{cm}^3$  and a propellant mass of 1.05kg, a total  $\Delta V$  of 128m/s will be provided without heating of the thrusters. Operation in warm gas mode is expected to raise the total  $\Delta V$  to over 160m/s with an overall power use of 10W. With the heating used to balance out non-ideal losses, a more conservative view of the warm gas mode assumes a total  $\Delta V$  of 135m/s for the ARAPAIMA mission.

### 3. Payload Science

The goal of the mission is to perform optical relative navigation with respect to the RSO with the purpose of demonstrating space-based SSA in a nanosat platform and in testing a novel method of obtaining 3D point clouds of the RSO using a single beam LRF [5]. This section describes a few topics of interest for visible and IR imaging and the proposed solution for generating 3D point clouds of the RSO.

Visible spectrum imaging and radiometric observations in the IR spectrum are of special interest to the ARAPAIMA team. Specifically, the team is interested in visible spectrum imaging of the RSO, during the day side of the orbit, for passive optical relative navigation with respect to it.

IR radiometry science, during the night side of the orbit, is of interest for the study of the differential cooling of an RSO after it transitions from the day side to the eclipse side of the orbit which could be used to investigate the remaining propellant in the tanks of the RSO. A related research topic is the capability to discriminate any active components of the RSO by observing their IR emissions.

For budget, power, and mass-constrained missions the simplicity and inherent reliability combined with its small size and low power make the LRF an attractive instrument for generating 3D point clouds by using the nanosat and its attitude motion as a scanning platform. Laser reflectance measurements of the LRF beam on the surface of the RSO are also of interest for material recognition and discrimination for future SSA missions.

#### 3.1. Payload Instruments

The ARAPAIMA payload instruments are an MLR2K LRF, a SenTech STC-CL232A visible spectrum camera, and a GA640C IR camera. Both cameras are monochrome. The payload instruments were chosen for their small size and relatively low power consumption and they are shown in Figure 7. Their specific features are discussed below. The measurement range of the LRF is 0 to 2km, its accuracy is 0.3m about the mean, at  $1\sigma$ , the maximum pulse repetition frequency (PRF) is 5Hz, and it operates at a wavelength of 1535nm. Its operating temperature range is  $-40^{\circ}\text{C}$  to  $63^{\circ}\text{C}$ . The IR camera is sensitive in the 900 to 1700nm range and the resolution of its InGaAs array is  $640 \times 512$  pixels. The IR camera does not require cooling. Its operating temperature range is  $-35^{\circ}\text{C}$  to  $71^{\circ}\text{C}$ . The STC-CL232A visible spectrum camera uses a CCD detector with  $1620 \times 1220$  pixels. The operating temperatures range from  $-5^{\circ}\text{C}$  to  $40^{\circ}\text{C}$ . Both cameras have CamLink interfaces for

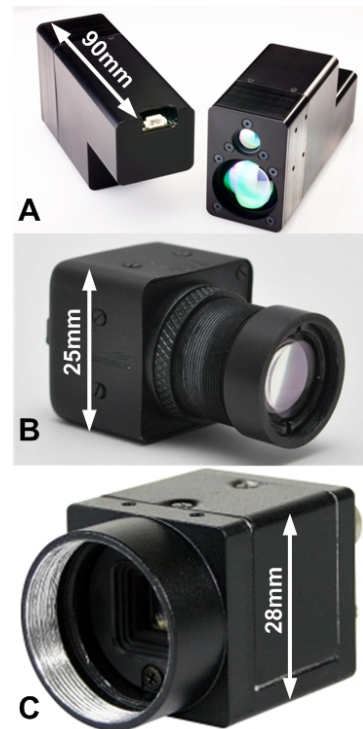


**Figure 7:** ARAPAIMA payload instruments. The MLR2K laser rangefinder (A), the GA640C SWIR camera (B), and the SenTech CL232A visible spectrum camera (C).

connection with a payload computer via frame grabbers.

### 3.2. Payload Experiments

The payload team conducted preliminary experiments with a suite of payload HW emulators for the purpose of retiring early the payload development and integration risks. A secondary objective was to train the students with hands-on projects and recruit the best ones for graduate studies.

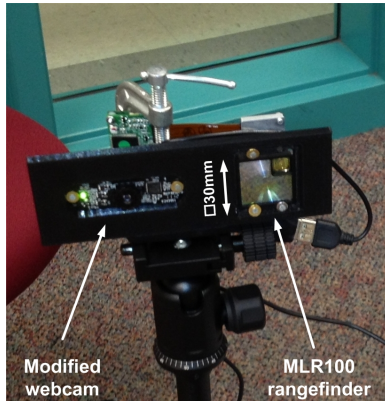


**Figure 8:** *Payload emulator experiment with the MLR100 rangefinder and a modified webcam.*

The payload emulator consists of the MLR100 miniature LRF from FLIR Systems, Inc., the manufacturer of the MLR2K chosen for ARAPAIMA, and a modified Logitech webcam which serves as an IR camera. The MLR100 LRF has a range of better than 100m and it operates at a wavelength of 905nm. The manufacturer stated accuracy of the MLR100 is “centimeter level” at  $1\sigma$ . The IR filter of the webcam was removed and replaced with a strip of exposed and developed color film which serves as a broadband filter. The students from the payload team have designed a mount for the LRF and the webcam and manufactured it on a 3D printer in the SDL.

Two experiments have been performed so far. One experiment consisted of a visual check of the LRF bloom from a terrestrial solar panel and an accuracy test of the LRF measurements for targets made of various materials. The results of the accuracy of the LRF were presented in [2].

The solar panel is a model from the SX series manufactured by BP, with solar cells made of polycrystalline silicon. The back of the solar panel is made of aluminum sheet painted white. The results of the visual reflectivity check experiment are shown in Figure 9. It can be noticed that the solar cells absorb most of the IR light of the laser and only the metalized space between the solar cells is seen by the modified webcam.

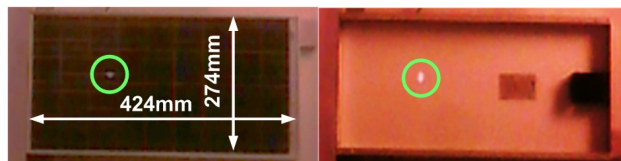


**Figure 9:** *Results of the visual check of the reflection of the laser light from the solar cells. Only the reflection from the metalized space between the solar cells is seen by the webcam (left) in contrast to the full bloom reflected by the white backside (right).*

On the other hand the oblong shape of the bloom, due to the strip laser diodes, can be easily seen on the white backside of the panel. It is important to emphasize that the solar cells on current satellites are typically triple junction, of  $\text{GaInP}_2$ , GaAs, and Ge, layered on the top of each other. Accordingly, the terrestrial solar panel is not a one-to-one representative of a modern spacecraft solar panel. In

addition, because the same material reflects light at various wavelengths differently the team notes that the emulator LRF emits a shorter wavelength than the flight LRF.

However, the team expects similar trends which will be verified by using the same test conditions with the payload instruments proposed for ARAPAIMA.

Integration of the payload computer with the frame grabber and the Linux operating system has also been addressed and the preliminary results are encouraging. An Active Silicon Phoenix frame grabber and its SW driver have been integrated with a VersaLogic CPU PC/104-Plus module. Preliminary tests with a SenTech STC-CL33A monochrome camera, with a resolution of  $648 \times 480$  pixels, have been conducted to check the operation of the integrated components. The STC-CL33A camera is used as a substitute for the IR camera for the payload integration work in the laboratory. An image captured with the camera is shown in Figure 10. The students working on the payload integration are actively cooperating with the SW engineers at Active Silicon Ltd. who are developing a major revision of the Linux drivers for the Phoenix frame grabbers.



**Figure 10:** *Image of the ADCS Lead Engineer captured with the integrated payload subsystem.*

#### **4. Science Phase Concept of Operations**

This section presents the detailed ConOps during the science phase of the mission, following RSO acquisition. A flow diagram that describes the major events and their dependencies is shown in Figure 11.

At this stage of mission planning it is assumed that the systems checkout lasts one week and it is planned that during checkout the nanosat performs a few orbital maneuvers that reduce the separation from the upper stage that is used as a surrogate RSO. A preliminary analysis shows that three OMT burns performed during checkout put the nanosat in an orbit that approaches a Minotaur IV Stage 4 at a rate of 10km/h, at an expense of  $1.8\text{m/s } \Delta V$ . It is assumed that the Minotaur IV upper stage orbits at 500km in a circular LEO.

The science checkout and proximity risk reduction begins at the end of the systems checkout phase. The nanosat is maneuvered, with commands loaded from the ground station, to perform station-keeping (SK) and enter natural motion circumnavigation (NMC) with respect to an “imaginary” RSO. The parameters of this first NMC are a cubic bounding box with an edge of 10km and a distance of 100km in the negative  $v_{\text{bar}}$  between the RSO and the center of the box. The notation for this NMC is  $10 \times 10 \times 10 \times (-100)\text{km}$  and it will be used throughout the section. The imaginary RSO is an orbital position which will be propagated on-board the nanosat and it will be used to safely verify the guidance algorithms. Waypoint navigation maneuvers that modify the NMC are performed to check the performance of both the algorithms and of the nanosat subsystems. A few orbit maintenance maneuvers, also called trim burns, are



to obtain autonomous relative pose estimation. A subphase goal of the mission is to test the algorithms in the highly dynamic conditions of LEO and collect imagery that can be used 1) on the ground for the verification and validation of new rel-nav algorithms and, 2) to provide data for worst-case lighting simulations for future GEO satellite servicing applications.

The nominal 250m radius circular orbit is the closest the nanosat is planned to approach the RSO. Imagery taken from the relative orbit allows the verification of a set of navigation algorithms which include “mono stereovision” or structure from motion, bounded Hough transform for relative pose estimation. The goal is subphase of the mission is to test the algorithms in the highly dynamic lighting conditions of LEO and collect imagery that can be used on ground for the verification and validation of new relative navigation algorithms.

A few of the science algorithms, such as the shape reconstruction from 3D point clouds and relative orbit navigation by waypoints have already been developed and tested in a simulation environment in MATLAB [7, 6, 5]. Other algorithms are currently being developed.

Last but not least, the extended mission includes the generation of guidance profiles using Inverse Dynamics in the Virtual Domain (IDVD). These real-time, near-optimal relative trajectories are calculated on-board, with constraints that would allow the nanosat to hover over a feature of interest of the RSO. If satellite jitter and navigation uncertainties allow it, several other experiments in collaboration with external researchers are also planned. For example, it is planned to use the LRF and relative orbital motion and attitude motion of the nanosat to scan and generate a point cloud of the RSO.

At the conclusion of the science experiments the nanosat will be commanded to reenter the atmosphere and deactivate.

## **5. Conclusions**

The ARPAIMA team has successfully passed the system concept review (SCR) in March 2013 and the system requirements review (SRR) in April 2013. Due to the highly dynamic nature of the project some of the requirements are still worked on and refined to better capture the flow-down from the top level mission requirements. The PDR is scheduled for mid August 2013 and the team is currently engaged in subsystem design and analysis and construction of a non-functional prototype of the nanosat.

Preliminary simulations have shown that the concept of operations is sound and the mission goals can be achieved. The difficulty of performing space-based SSA with a nanosat is fully recognized and work is planned to reduce the mission risks at an early stage.

The team acknowledges the support of the AFRL UNP Program Office and that of the Embry-Riddle Aeronautical University College of Engineering and the Department of Aerospace Engineering.

## References

- [1] Department of Defense Instruction 3100.12 - Space Support. DoD, Sep. 2000.
- [2] A. Harris, K. Baba, DiGregorio J., Grande T., Castillo C., Zuercher T., Udrea B., and Nayak M. V. Experimental characterization of a miniature laser rangefinder for resident space object imaging. In *2013 AAS Space Flight Mechanics Conf.*, Kauai, HI, Jan. 2013.
- [3] A. Huang and E.-H. Yang. MEMS-based warm gas thruster system for cubesat orbital maneuver applications. In *SPIE Space Exploration Technologies II Conference*, Orlando, FL, Aug. 2010. Paper 7331–15 (Invited Speaker).
- [4] R. Moore, W. Holemans, A. Huang, J. Lee, M.G. McMullen, J. White, R. Twiggs, B. Malphrus, N. Fite, D. Klumpar, E. Mosleh, K. Mashburn, D. Wilt, J. Lyke, S. Davis, W. Bradley, T. Chiasson, J. Herble, and P. Patterson. 3d printing and MEMS propulsion for the RAMPART 2U CubeSat. In *Small Sat Conference*, Logan, UT, Aug. 2010. Paper , SSC10-III-8.
- [5] M. V. Nayak, Udrea B., Marsella B., and Beck J. Application of a laser rangefinder for space object imaging and shape reconstruction. In *2013 AAS Space Flight Mechanics Conf.*, Kauai, HI, Jan. 2013.
- [6] M. V. Nayak, Beck J., and Udrea B. Closed-loop attitude control for generation of high density point clouds of resident space objects with a laser rangefinder. In *34th IEEE Aerospace Conference*, Big Sky, MT, Mar. 2013.
- [7] M. V. Nayak, Beck J., and Udrea B. Design of relative motion and attitude profiles for three-dimensional resident space object imaging with a laser rangefinder. In *34th IEEE Aerospace Conference*, Big Sky, MT, Mar. 2013.